



Original scientific paper

Electrochemical mediated oxidation of phenol using Ti/IrO₂ and Ti/Pt-SnO₂-Sb₂O₅ electrodes

Jéssica Pires de Paiva Barreto, Elisama Vieira dos Santos, Mariana Medeiros Oliveira, Djalma Ribeiro da Silva, João Fernandes de Souza* and Carlos A. Martínez-Huitle[✉]

Federal University of Rio Grande do Norte, CCET - Institute of Chemistry, Campus Universitario, Lagoa Nova - CEP 59.072-970, RN, Brazil

*Federal University of Rio Grande do Norte, CCET – Department of Chemical Engineering, Campus Universitario, Lagoa Nova - CEP 59.072-970, RN, Brazil

[✉]Corresponding Author: E-mail: carlosmh@quimica.ufrn.br; Tel.: +55-84-9181-7147;

Received: October 13, 2014; Published: December 6, 2014

Abstract

The indirect electrochemical oxidation of phenol was studied at Ti/IrO₂ and Ti/Pt-SnO₂-Sb₂O₅ electrodes by bulk electrolysis experiments under galvanostatic control. The obtained results clearly shown that the electrode material was an important parameter for the optimization of such processes determining their mechanism and oxidation products. Different current efficiencies were obtained at Ti/IrO₂ and Ti/Pt-SnO₂-Sb₂O₅, depending on the applied current density in the range from 10, 20 and 30 mA cm⁻². The effect of the amount of dissolved NaCl was studied also. It was observed that the electrochemical processes (direct/indirect) favor specific oxidation pathways depending on electrocatalytic material. Phenol degradation generates several intermediates eventually leading to complete mineralization, as indicated by the results obtained with the High-performance liquid chromatography (HPLC) technique.

Keywords

Phenol; anode material; chlorine active species; indirect electrochemical oxidation.

Introduction

Phenol is an aromatic compound and it is a hygroscopic crystalline solid at ambient temperature and pressure. When pure, solid phenol is white but is mostly colored due to the presence of impurities. Phenol is very soluble in ethyl alcohol, in ether and in several polar solvents, as well as in hydrocarbons such as benzene. In water it has a limited solubility and behaves as a weak acid [1]. More phenol than is usually found in the environment has been found in surface waters and

surrounding air that were contaminated when phenol was released from industries and commercial products containing phenol. It has been found in materials released from landfills and hazardous waste sites, and it has been found in the groundwater near these sites [2,3].

The interest in developing new and more efficient methods for destruction of hazardous waste such as phenol [4] and the conversion of mixed waste to low-level-toxicity waste has significantly increased. These wastewaters are difficult to be effectively treated by conventional biological methods, for this reason, advanced oxidation processes (AOPs) have been developed to treat these bio-refractory organic wastewaters [1-11]. In this frame, the electrochemical oxidation of the model substrates has been investigated using several anodic materials, generally metal oxides like IrO_2 , PbO_2 , SnO_2 and $\text{SnO}_2\text{-Sb}_2\text{O}_5$ [5,6]. Dimensionally stable anodes (DSAs) belong to a particular category of electrodes, constituted of a Ti-support coated by noble metal oxides, which confer the enhanced catalytic activity towards chlorine evolution and oxygen evolution reaction (o.e.r). To date, DSAs have been largely employed in the chloro-alkali industry, due to their excellent catalytic property and service life [12,13]; however, significant performances have been obtained when these have been used for electrochemical treatment of industrial effluents [14].

In the case of active chlorine, the interest in this oxidant is based on the ubiquitous presence of chloride ions in a certain number of effluents and natural waters, making possible the involvement of active chlorine during electrochemical treatment using principally DSA electrodes; and the chemistry and electrochemistry of higher oxidation states for chlorine close to neutral pH [15,16].

The electrochemical treatment of phenol has been already studied by other authors [2-4,9-11, 17,18]. Using NaCl solutions to degradate phenol by direct anodic reaction and/or through the mediation of active chlorine [19,20]; the possible role of the Cl^- ion during the process was not taken into account by the authors [19,20]. Therefore, the electrochemical degradation of phenol was studied at Ti/IrO_2 and $\text{Ti/Pt-SnO}_2\text{-Sb}_2\text{O}_5$ electrodes by varying operating conditions such as current density and Cl^- concentration. The intermediate species formed at each one of the anodes were compared.

Experimental

Chemicals

The compounds used such as phenol, catechol, hydroquinone, oxalic acid were of analytical grade. The chromatographic elution solvents were of HPLC grade (Merck). The stock solutions (1000 mg L^{-1}) of phenol and its degradation products were prepared from certified reference standards (purity > 98 %), with the dissolution in methanol HPLC grade. All electrolyte solutions were prepared using purified Milli-Q water system with a conductivity of $0.1 \mu\text{S cm}^{-1}$.

Electrochemical measurements

Electrochemical analyses were performed with an Autolab model PGSTAT320N (Metrohm). Quasi-steady polarization curves were carried out at a scan rate of 2.5 mV s^{-1} and with a 0.45 mV step potential, in solutions of NaCl at different concentrations. Experiments were carried out in a conventional three-electrode system, and measurements were performed in a range from 0.0 V to 3.5 V . Ti/IrO_2 and $\text{Ti-Pt-SnO}_2\text{-Sb}_2\text{O}_5$, with an exposed geometric area of ca. 1.0 cm^2 , were used as the working electrode, while a platinum wire and an Ag/AgCl ($\text{KCl } 3 \text{ mol L}^{-1}$) electrode were employed as the auxiliary and reference electrodes, respectively.

Electrolytic systems

Bulk oxidations were performed in an electrolytic flow cell with a single-compartment with parallel plate electrodes [21]. Circular electrodes (Ti/IrO₂ and Ti-Pt-SnO₂-Sb₂O₅ electrode) were used as anodes exposing to the effluent a nominal surface area of 63.5 cm². In all cases, a Ti disc was used as the cathode. The inter-electrode gap was 10 mm. For the electrochemical flow cell, inlet and outlet were provided for effluent circulation through the reactor; the solution of phenol was stored in a thermoregulated glass tank (1 L) and circulated through the cell using a peristaltic pump, at a flow rate of 151 dm³ h⁻¹, which allowed a mass transfer coefficient (determined using the ferri/ferro-cyanide redox couple) of 2.0×10⁻⁵ m s⁻¹ [22]. The oxidation experiments of phenol were performed under galvanostatic conditions (using a power supply MINIPA-3305M) at 25 °C for studying the role of applied current density ($j = 10, 20$ and 30 mA cm^{-2}) adding 20 and 30 mM of Cl⁻ for studying the effect of Cl-mediated approach.

Analytical methods

The oxidation intermediates, produced during the electrolysis experiments at both anodes, were analyzed by HPLC. Chromatographic separations were performed on an analytical column Supelcosil-C18 (5 μm, 25 × 46 mm) at room temperature and with an UV detector at λ = 225 nm. Generated carboxylic acids were detected and quantified using an Ultimate TMAQ- C18 5 m (25 × 46 mm) column at room temperature and photodiode array detector set at λ = 210 nm. For these analyses, a 70:30 (v/v) methanol/water mixture at 0.5 mL min⁻¹ for the elution was used. The flow rate of the mobile phase was 1.5 mL min⁻¹. Spectrophotometric measurements (UV-Vis) were also performed using a Shimadzu model UV-160 spectrophotometer. Experimentally, degradation of phenol was monitored from the abatement of their chemical oxygen demand (COD). Values were obtained, using a HANNA HI 83099 spectrophotometer after digestion of samples in a HANNA thermo-reactor, in order to estimate the Total Current Efficiency (TCE), using the following relationship [23]:

$$\text{TCE, \%} = FV \left(\frac{[\text{COD}_0 - \text{COD}_f]}{8I\Delta t} \right) \times 100 \quad (1)$$

where COD₀ and COD_f are chemical oxygen demands at times $t=0$ (initial) and f (final time) in g O₂ dm⁻³, respectively; I the current (A), F the Faraday constant (96,487 C mol⁻¹), V the electrolyte volume (dm³), 8 is the oxygen equivalent mass (g eq.⁻¹) and Δt is the total time of electrolysis, allowing for a global determination of the overall efficiency of the process. Additionally, the limiting current can be estimated from the value of COD using the equation 2 for electrochemical oxidation of phenol [24,25].

$$I_{\text{lim}}(t) = 4FAk_m \text{COD}(t) \quad (2)$$

where $I_{\text{lim}}(t)$ is the limiting current (A) at a given time t , 4 the number of exchanged electrons, A the electrode area (m²), F the Faraday's constant, k_m the average mass transport coefficient in the electrochemical reactor (m s⁻¹) and COD(t) the COD, mol O₂ m⁻³ at a given time t .

The energy consumption (EC) per volume of phenol oxidized was estimated and expressed in kWh dm⁻³. The average cell voltage, during the electrolysis, is taken for calculating the energy EC, as follows:

$$\text{Energy consumption} = \frac{\Delta E_c I t}{3600V} \quad (3)$$

where t is the time of electrolysis (s); $\Delta E_c / V$ and I / A are the average cell voltage and the electrolysis current, respectively; and V is the sample volume (dm^3).

Results and discussion

Polarization curves in the presence of halide

Based on the considerations about the possible effect of halide on the oxygen evolution reaction (o.e.r.) polarization curves were recorded in the absence and in the presence of different concentrations of Cl^- . The results obtained in the presence of chloride ions (10 to 80 mg L^{-1}), at both anode materials, are shown in Fig. 1. In the case of the Ti/IrO_2 anode, in absence of chloride in solution, the oxygen evolution reaction is attained around 1.7 V. After that, the whole polarization curve is modestly shifted to less positive potentials (up to 1.5 V), when the concentration of NaCl is increased. This behavior is due to the increase of the importance of the $\text{Cl}_2/\text{H}_2\text{O}$ system [23,26], favoring the production of active chlorine species than the oxygen evolution reaction. Under these conditions, a fast incineration of a number of organic substrates can be favored during mediated electrochemical process due to the production of oxychloro-radicals, often assumed as intermediates in the chlorine evolution reaction.

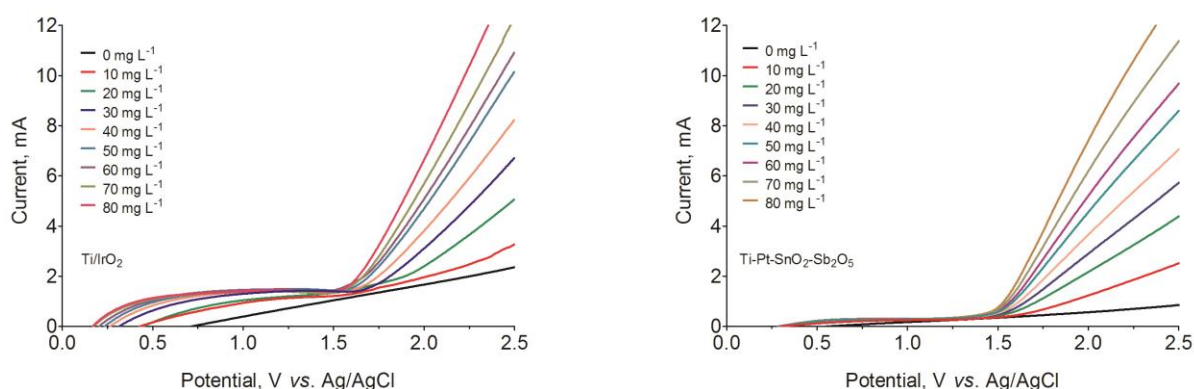


Figure 1. Current-potential curves in the presence of different amounts of NaCl on Ti/IrO_2 and $\text{Ti-Pt-SnO}_2\text{-Sb}_2\text{O}_5$ anodes at scan rate of 2.5 mV s^{-1} . Black curve: Water with lower conductivity.

Similar experiments were carried out using $\text{Ti-Pt-SnO}_2\text{-Sb}_2\text{O}_5$ anode in the presence of Cl^- , as shown in Fig. 1, employing the same range of Cl^- concentrations. In that case, at very small NaCl concentration (10 mg L^{-1}), a relevant shift to less positive potentials was observed of I/E curves. Above 20 mg L^{-1} , the anode potential becomes increasingly buffered by the halide electroactivity. This behavior can be attributed to an interaction between anode surface and Cl^- to form active chlorine species (desirable and undesirable, such as Cl^\bullet , Cl_2 , ClO_2^- and ClO_3^- , ClO_4^- , respectively) with this active material [16]. According to the electrode nominal composition, it suggests a mix-behavior as active or non-active anode due to the presence of SnO_2 in its surface. In fact, the oxygen evolution reaction is achieved at more positive potentials than that observed at Ti/IrO_2 anode. However, the performances of $\text{Ti-Pt-SnO}_2\text{-Sb}_2\text{O}_5$ anode are not comparable with the performance of an ideal non-active anode like diamond electrode [26]. It indicates that, the concentration of halide in solution increases the importance of $\text{Cl}_2/\text{oxy-chloro}$ radicals system depending on the electrocatalytic material and this behavior plays an important role in relation with the oxygen evolution reaction, influencing on the efficiency of electrochemical approach adopted [27-29].

Bulk electrolysis

The experiments were performed at 25 °C varying Cl^- concentration ions (20 and 30 mM) in solution and applied different current density (10, 20 and 30 mA cm^{-2}) in order to evaluate the elimination of organic load. Fig. 2 shows the performances of each one of the electrocatalytic material used as a function of applied current density and electrolyte concentration during the COD removal. It was observed that efficiency of COD removal was dependent on the applied current density and Cl^- concentration. In fact, when 10, 20 and 30 mA cm^{-2} were applied by using Ti/IrO_2 , the initial COD (338 mg L^{-1}) was reduced 262 mg L^{-1} ; 182 mg L^{-1} and 140 mg L^{-1} with 20 mM of Cl^- in solution, while at 30 mM of Cl^- , COD decays to 193 mg L^{-1} , 123 mg L^{-1} and 121 mg L^{-1} for 10, 20 and 30 mA cm^{-2} , respectively, after 120 min of electrolysis. For $\text{Ti-Pt-SnO}_2\text{-Sb}_2\text{O}_5$ anode, under similar conditions, COD concentration was reduced from 338 mg L^{-1} to 223, 45 and 96 mg L^{-1} at 20 mM of Cl^- and 158; 18 and 98 mg L^{-1} when 30 mM of Cl^- was added by applying 10, 20 and 30 mA cm^{-2} , respectively.

Based on the COD removal reported in Fig. 2, the increase in the applied current density contributes to the degradation of phenol and the intermediates generated during the electrolysis, thanks to the action of active chlorine species produced on the electrodes surface. However, the results reveal that at $\text{Ti-Pt-SnO}_2\text{-Sb}_2\text{O}_5$ there is greater reduction in COD than that achieved at Ti/IrO_2 (Fig. 2), principally at 20 mA cm^{-2} . Conversely, when 30 mA cm^{-2} was applied, the elimination of COD decreased due to the promotion of Cl_2 rather than the production of active chlorine species.

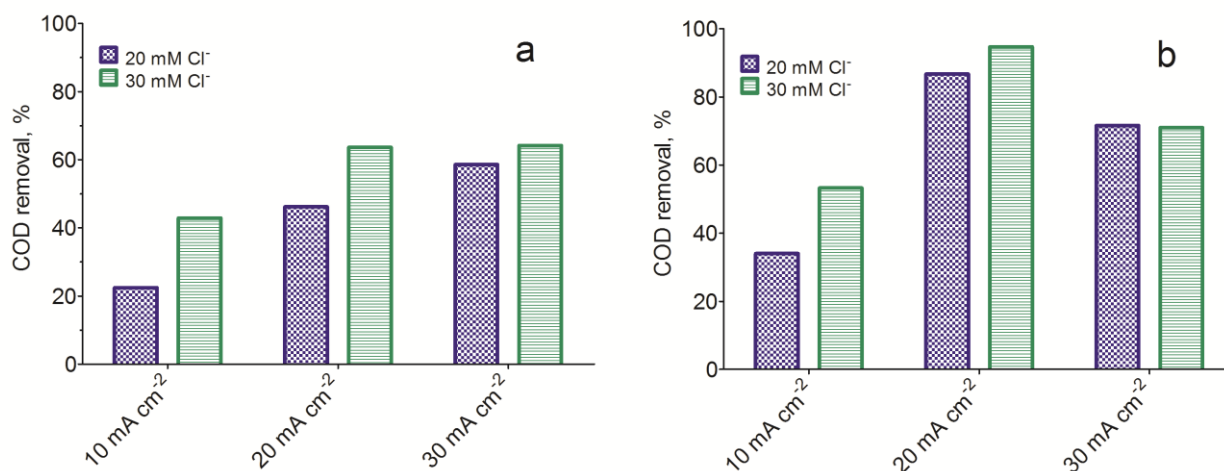
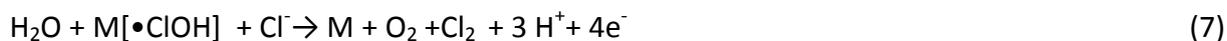


Figure 2. Effect of NaCl for COD removal at different concentrations during mediated electrochemical oxidation of phenol by using (a) Ti/IrO_2 and (b) $\text{Ti-Pt-SnO}_2\text{-Sb}_2\text{O}_5$ anodes. Operational conditions: $[\text{Phenol}]_0 = 100 \text{ mg L}^{-1}$, initial COD = 338 mg L^{-1} , $T = 25^\circ\text{C}$.

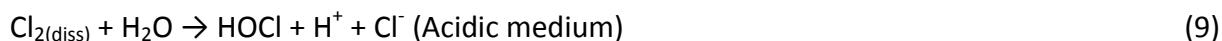
This behavior suggests that phenol oxidation depends on the nature of the anode material due to the efficient production of active chlorine species on anode surface [23, 26-29]. Ti/IrO_2 and $\text{Ti-Pt-SnO}_2\text{-Sb}_2\text{O}_5$ materials are classified as active anodes [5,6] because these electrocatalytic materials are characterized by strong electrode-hydroxyl radical interaction, resulting in a low chemical reactivity for organics oxidation. This problem can be avoided when Cl-mediated approach is used [14]. Generally, under favorable pH conditions and NaCl in solution, electrochemical oxidation via $\bullet\text{OH}$ radicals is not the only oxidation mechanism that occurs on the DSA anodes [14]. In this case, chlorohydroxyl radicals are also generated on anode surface and consequently oxidizing organic matter (Equations 4 and 5) [30,31]:



Reactions between water and radicals near to anode surface can yield molecular oxygen, free chlorine, and hydrogen peroxide (6, 7 and 8) [32]:



Furthermore, hypochlorite can be formed as follows (9 and 10) [31]:



Therefore, indirect oxidation results in reduction of organic pollutants such as phenol thanks to the participation of active chlorine species electrochemically formed [15,23,31]. Oxidants are quite stable and migrate in the solution bulk, and then, these indirectly oxidize the effluent, favored by hydrodynamic configuration of electrochemical cell. The efficiency of indirect oxidation depends on the diffusion rate of oxidants in the solution, concentration of oxidants, and pH of solution [15].

For the electrochemical flow cell used in this study, the mass transfer coefficient was $2.0 \times 10^{-5} \text{ m s}^{-1}$, and the limiting current (for both anodes) results in an average value of 0.88 A, according to Eq. 2. This current is lower than all the currents applied in this work (1.27–1.90 A), suggesting that the oxidation under these experimental conditions could occur under mass transport control since 120 min of electrochemical treatment. These assumptions are in agreement with the studies published by Cañizares and co-workers [33].

UV spectroscopic characteristics of the electrochemical oxidation of phenol

The oxidation of phenol at Ti/IrO₂ and Ti-Pt-SnO₂-Sb₂O₅ electrodes was also monitored by spectrophotometric measurements, which allow a straightforward way to follow the elimination of phenol. Thus, UV spectra for phenol degradation at Ti/IrO₂ and Ti-Pt-SnO₂-Sb₂O₅ electrodes, at 20 mM and 30 mM of Cl⁻ in solution at 25°C by applying 20 mA cm⁻², are shown in Figure 3. An inspection of these UV spectra allowed confirming that phenol was more rapidly removed at Ti/IrO₂ (Fig. 3a and 3b, at 20 mM and 30 mM of Cl⁻ in solution by applying 20 mA cm⁻²) than at Ti-Pt-SnO₂-Sb₂O₅ electrodes under the same experimental conditions (Fig. 3c and 3d). Moreover, the bands in Fig 3a and 3b are completely different after 5 minutes of electrolysis due to formation of reaction intermediates, confirming the fast degradation of phenol. These major changes in UV- vis bands are not observed in Figs. 3c and 3d. This behavior depends on the effective electrochemical production of active chlorine species at both anodes. Perhaps, at IrO₂, metal cations in the oxide lattice may reach higher oxidation states under anodic polarization stabilizing •OH radicals and Cl⁻ ions on its surface [6,32,34], which favors the O₂ and Cl₂ evolution at the expense of the electrochemical incineration reaction. This feature avoids the formation of enough active chlorine species that promote an efficient degradation of phenol, generating different aromatic intermediates. However, it is not possible to reliably ensure that phenol is degraded because the products and/or intermediates formed during the process may have a higher molar absorptivity (ϵ) and absorb in the same wavelength region of phenol.

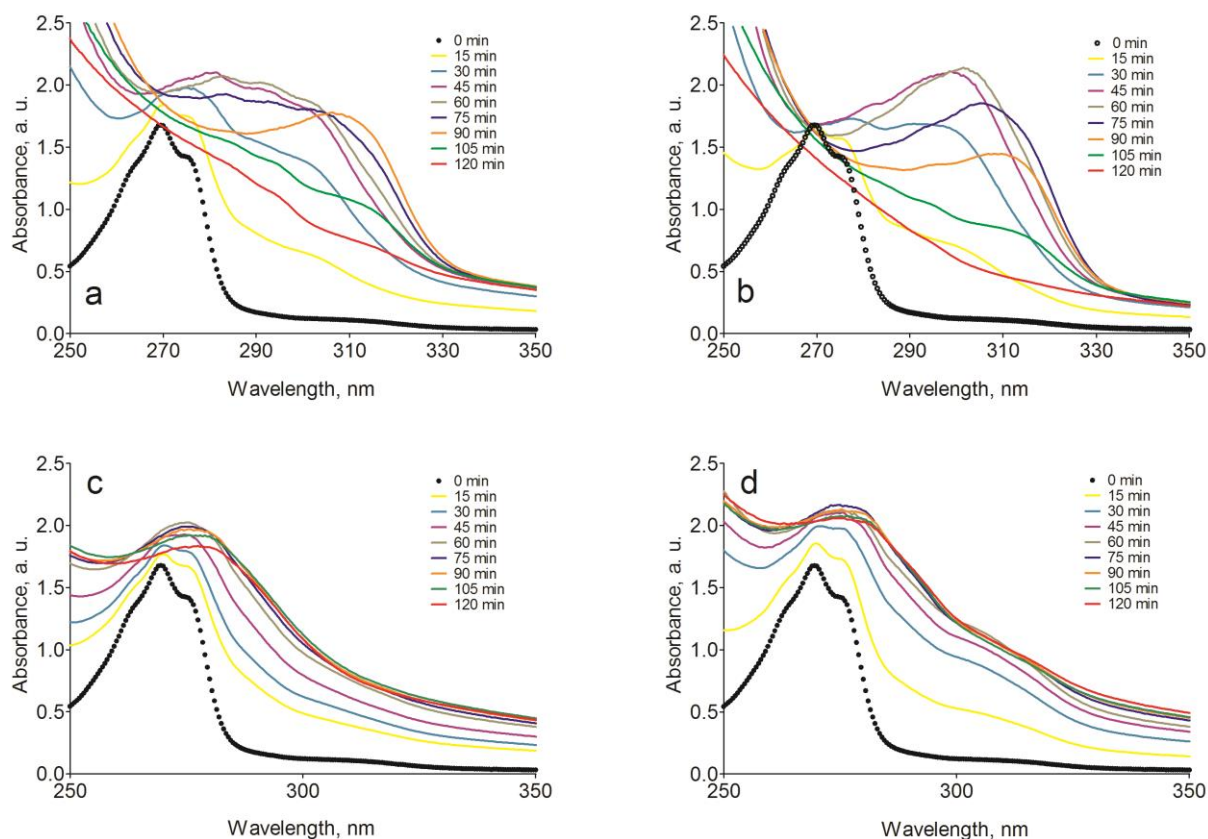


Figure 3. Spectrophotometric measurements, as a function of time, during Cl-mediated electrochemical treatment of phenol (100 mg L^{-1}) by applying 20 mA cm^{-2} at 25°C . Ti/IrO₂: (a) 20 mM of Cl⁻ and (b) 30 mM of Cl⁻. Ti-Pt-SnO₂-Sb₂O₅: (c) 20 mM of Cl⁻ and (d) 30 mM of Cl⁻.

Conversely, at Ti-Pt-SnO₂-Sb₂O₅ electrode (Fig. 3c and 3d), the elimination of phenol is attained by the reactive chlorine species such as chlorine and hypochlorous acid or hypochlorite ion (Cl₂, HClO and OCl⁻) that react rapidly with organics mainly by the reactions in solution [23,35,36]. In acidic conditions, free chlorine is the dominant oxidizing agent, while in slightly alkaline conditions hypochlorite, chloride ions and hydroxyl radicals are all generated in relevant concentrations [26,31]. In fact, pH typically varies between 5.5 and 6.2 throughout the course of the reaction for phenol. Then, this pH behavior suggests the participation of active chlorine oxidants, confirming the increase on COD removal rate when Ti-Pt-SnO₂-Sb₂O₅ electrode was used.

Distribution of by-products of phenol oxidation

As stated above, phenol could be transformed into different intermediates or carbon dioxide during the process and such differences would not be apparent from the time- or charge-course of this parameter. For this reason, identification of some intermediates was performed by HPLC. The change in concentration of phenol (initial concentration of 100 mg L^{-1}) and intermediates in the course of indirect electrochemical treatment, by applying 20 mA cm^{-2} at 25°C , is shown in Fig. 4a-d. As can be observed, the degradation of phenol (main by-product formed) is influenced by the amount of Cl⁻ as well as the electrocatalytic material used. In fact, 84 % and 88 % of phenol was removed by using Ti/IrO₂ anode after 120 min of electrolysis when 20 and 30 mM of Cl⁻ in solution were used, respectively. Conversely, the decrease of phenol on Ti-Pt-SnO₂-Sb₂O₅ was about 93 % and 83 % by applying 20 mA cm^{-2} for 20 and 30 mM of Cl⁻, respectively. As shown in Fig. 4, the intermediates concentration produced on Ti/IrO₂ and Ti-Pt-SnO₂-Sb₂O₅ electrodes are different.

Hydroquinone, which is aromatic intermediate, was principally found in high concentration at the experiments performed with Ti/IrO₂ anode. HPLC results indicated the transformation of the phenol by electrolysis to hydroquinone, which was decomposed to other forms. This behavior was observed at both anodes where similar by-products were formed. However, at Ti-Pt-SnO₂-Sb₂O₅, all the intermediates are quasi-completely mineralized to CO₂ and H₂O due to the attack of active chlorine species.

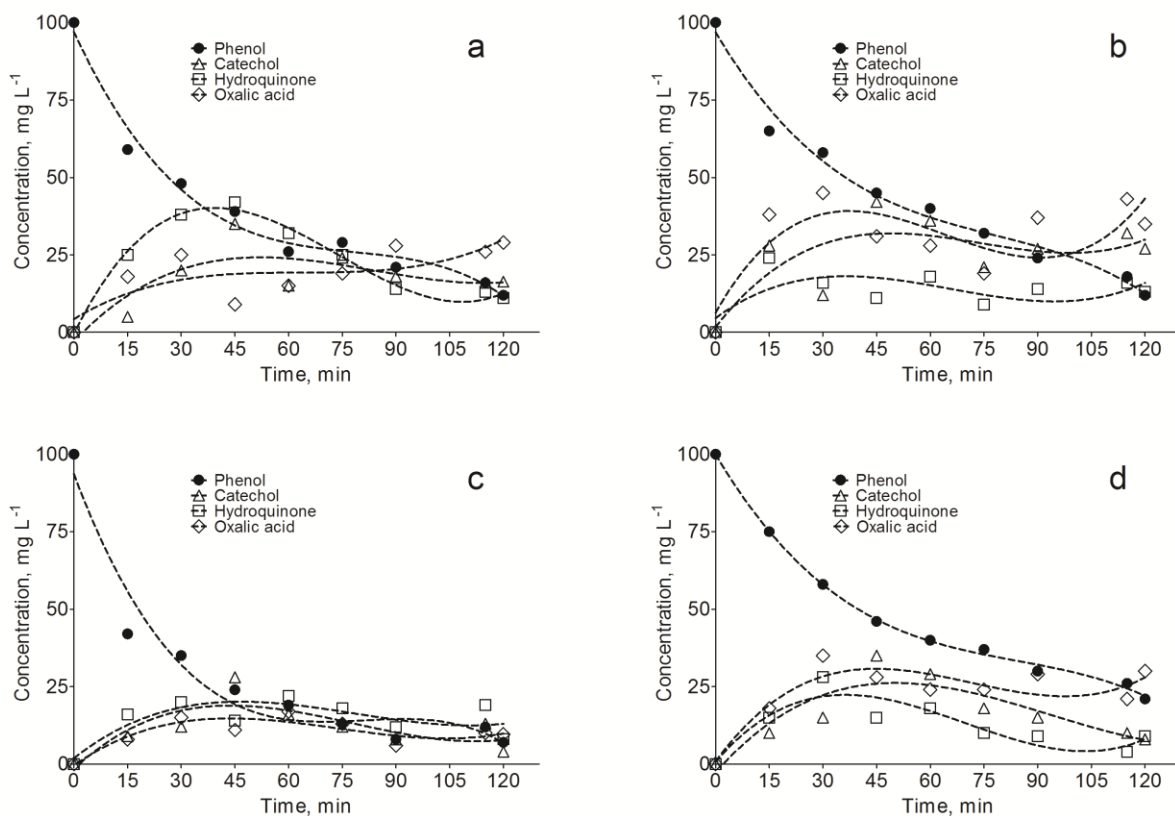


Figure 4. Intermediates formed during Cl-mediated oxidation of phenol (100 mg L^{-1}) by applying 20 mA cm^{-2} using Ti/IrO₂ ((a) 20 mM of Cl⁻ and (b) 30 mM of Cl⁻) and Ti-Pt-SnO₂-Sb₂O₅ ((c) 20 mM of Cl⁻ and (d) 30 mM of Cl⁻) anodes. HPLC retention times: benzoquinone: 1.9 min, catechol: 3.05 min; phenol: 3.5 min; hydroquinone: 2.76 min and oxalic acid: 2.3 min.

Moreover, it is found that the amount of oxalic acid produced on Ti-Pt-SnO₂-Sb₂O₅ is larger than that at Ti/IrO₂, suggesting a better grade of mineralization. It is important to indicate that, unidentified intermediates were produced; however, these by-products were predominantly generated at Ti/IrO₂ as showed by their chromatographic area (Fig. 5). For Ti/IrO₂, aromatic compounds concentration is not reduced with the action of active chlorine, finding difficult to break the aromatic ring and favoring the conversion of phenol to other aromatic compounds. Based on the results obtained, the effect of NaCl on Ti-Pt-SnO₂-Sb₂O₅ is much more evident and efficient to produce strong oxidants that promote the mineralization of phenol and by-products on the bulk of solution.

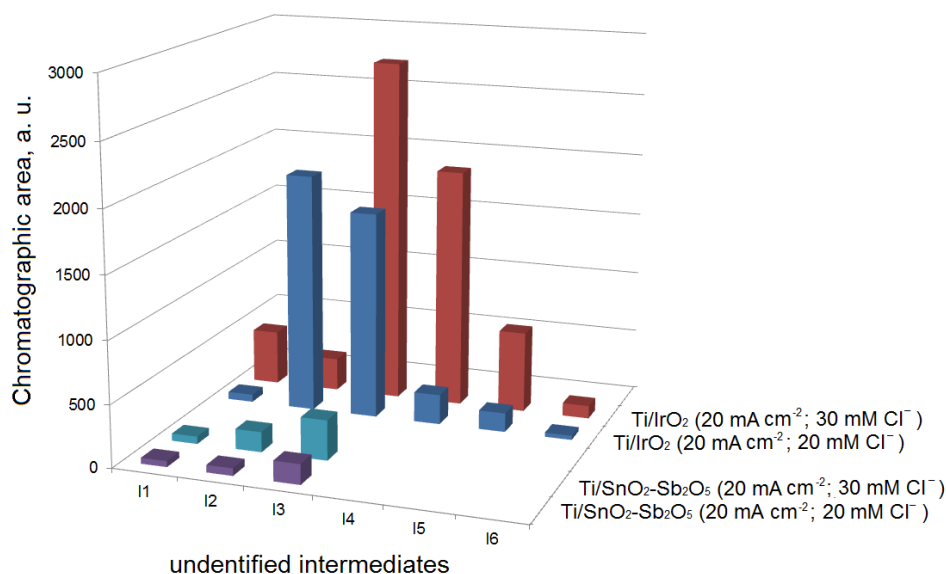


Figure 5. Chromatographic areas of unidentified intermediates produced during indirect electrochemical oxidation of phenol at Ti/IrO_2 (20 mM of Cl^- and 30 mM of Cl^-) and $\text{Ti-Pt-SnO}_2\text{-Sb}_2\text{O}_5$ (20 mM of Cl^- and 30 mM of Cl^-) anodes.

Kinetic and activation energy analysis

To study the kinetics of the overall reaction involved in the disappearance of phenol and intermediates by indirect electrochemical oxidation, the decay of phenol concentration under different NaCl concentration of electrolyte was considered. Results given in Fig. 6a and 6b were further analyzed using kinetic equations related to different reaction orders. Good linear plots were fitted to a pseudo-first-order reaction ($\ln(C_0/C_t)$ vs. time) for Ti/IrO_2 and $\text{Ti-Pt-SnO}_2\text{-Sb}_2\text{O}_5$ electrodes. For Ti/IrO_2 , apparent constant rates (k_{app}) of 0.020 min^{-1} ($r^2 = 0.97$) for 20 mM of Cl^- and 0.015 min^{-1} ($r^2 = 0.95$) for 30 mM of Cl^- were estimated; while for $\text{Ti-Pt-SnO}_2\text{-Sb}_2\text{O}_5$, 0.027 min^{-1} ($r^2 = 0.97$) for 20 mM of Cl^- and 0.017 min^{-1} ($r^2 = 0.98$) for 30 mM of Cl^- were achieved. These figures confirm that the indirect electrochemical oxidation is faster at $\text{Ti-Pt-SnO}_2\text{-Sb}_2\text{O}_5$ anode, respect to the behavior attained at Ti/IrO_2 , where the process is disfavored when an increase in Cl^- ion is performed. It can be due to the preferential production of Cl_2 gas, as discussed on polarization curves results [26]. In this form, lower concentrations of active chlorine are produced, favoring the electrochemical conversion of phenol to aromatic compounds. Considering the kinetic model pseudo-second order ($(1/C_0)-(1/C_t)$ vs. time) and concentration Cl^- ions in the medium, these show suitable linearity when compared to pseudo-first order model.

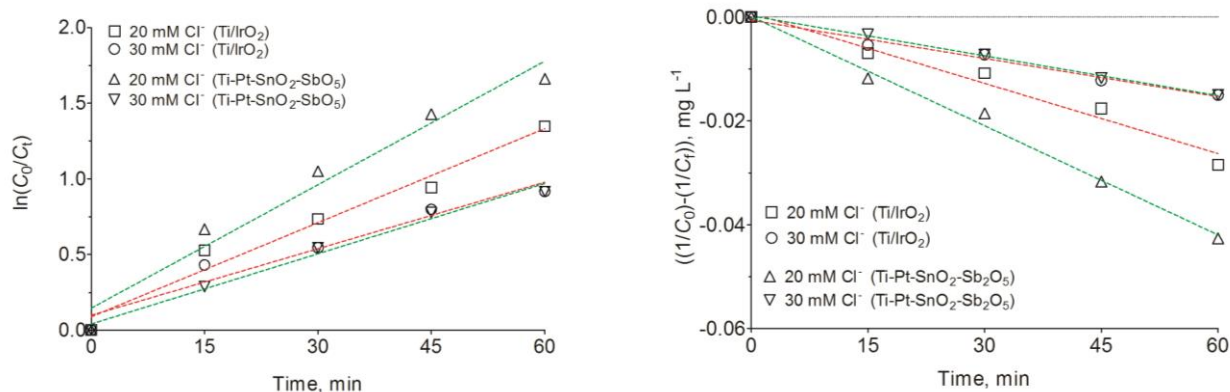


Figure 6. Kinetic analysis for the pseudo-first-order $\ln(C_0/C_t)$ and pseudo-second-order $(1/C_0)-(1/C_t)$ reaction for phenol decay during its indirect electrochemical oxidation by active chlorine species.

The coefficients of pseudo-second order were about $7.01 \times 10^{-4} \text{ min}^{-1}$ ($r^2 = 0.99$) and $2.5 \times 10^{-4} \text{ min}^{-1}$ ($r^2 = 0.99$) for concentration 20 and 30 mM of Cl^- , respectively, using Ti-Pt-SnO₂-Sb₂O₅. Conversely, values of $4.5 \times 10^{-4} \text{ min}^{-1}$ ($r^2 = 0.97$) and $2.4 \times 10^{-3} \text{ min}^{-1}$ ($r^2 = 0.98$) at concentration 20 and 30 mM of Cl^- were estimated at Ti/IrO₂ electrode. Then, the kinetic data obtained by pseudo-second order model indicate that the indirect oxidation is controlled by the rate at which organic molecules are carried from the bulk to the electrode surface, but when the concentration of final intermediates increase, their rate is limited by diffusion control. However, the principal step for the electrochemical approach is the production of active chlorine species, as indicated by pseudo-second order model.

Finally, it is very important to estimate the treatment applicability, and thus, Table 1 reports the current efficiency and energy consumption (kWh dm^{-3}) at 10, 20 and 30 mA cm^{-2} , after 120 min of electrochemical treatment. As can be observed, Ti-Pt-SnO₂-Sb₂O₅ consumed relatively less electrical energy than Ti/IrO₂ anode, but different current efficiencies were achieved after 120 min of electrolysis at both anode materials.

Table 1. Energy requirements and total current efficiency for elimination of phenol at different applied current densities by Cl-mediated electrochemical oxidation.

Current density, mA cm^{-2}	Current total efficiency, %		Energy consumption, kWh dm^{-3}	
	Ti/IrO ₂	Ti-Pt-SnO ₂ -Sb ₂ O ₅	Ti/IrO ₂	Ti-Pt-SnO ₂ -Sb ₂ O ₅
10	59	72	36	28
20	39	56	42	40
30	26	49	69	54

Conclusions

The Cl-mediated electrochemical oxidation of phenol was investigated under galvanostatic conditions at Ti/IrO₂ and Ti-Pt-SnO₂-Sb₂O₅ electrodes, as a function of applied current density and amount of NaCl dissolved. A partial elimination of the organic pollutant was achieved at Ti/IrO₂, while a quasi-complete electrochemical elimination takes place at Ti-Pt-SnO₂-Sb₂O₅ anode. The influence of the anode material on the elimination of phenol seems to be very important due to an efficient production of active chlorine species during electrolysis. In fact, Ti-Pt-SnO₂-Sb₂O₅ showed good electrocatalytic activity to promote the electrochemical generation of active chlorine, as indicated by potentiodynamic measurements, and as a consequence of this characteristic, significant removal efficiency of phenol and its by-products was attained.

The effect of chloride on the electrooxidation of organics with Ti/IrO₂ and Ti-Pt-SnO₂-Sb₂O₅ depends mainly on the reaction between electrogenerated $\bullet\text{OH}$ and Cl^- ions or the conversion of chloride ion to chlorine which is further hydrolyzed to other active species [26,37]. At the same time, the production of Cl^- to active chlorine is directly related to different experimental conditions, but it is principally dependent on the concentration of free $\bullet\text{OH}$ radicals, the increase of the importance of the $\text{Cl}_2/\text{H}_2\text{O}$ system and the interaction of Cl^- and $\bullet\text{OH}$ radicals with the anode surface. Because, increasing the concentration of Cl^- ions in solution, elimination of Cl^- from solution by Cl_2 is favored [23,37,38].

Acknowledgements: E. V. dos S. gratefully acknowledges the Programa de Recursos Humanos – PETROBRAS (PBFRRH-22) for her PhD fellowship and support provided by the Núcleo de Processamento Primário e Reuso de Água Produzida e Resíduos (NUPPRAR-UFRN) for analyzing the

samples electrochemically treated. The authors thank the financial support provided by CNPq and PETROBRAS. They also thank to the Dott. Christian Urgghe (Industrie De Nora S.p.A. - Milan, Italy) for providing Ti/IrO₂ and Ti-Pt-SnO₂-Sb₂O₅ electrodes.

References

- [1] J. E. Amore, E. Hautala, *Journal of Applied Toxicology* **3** (1983) 272–290.
- [2] Y.-q. Wang, B. Gu, W.-l. Xu, *Journal of Hazardous Materials* **162** (2009) 1159-1164.
- [3] M. Pimentel, N. Oturan, M. Dezotti, M. A. Oturan, *Applied Catalysis B: Environmental* **83** (2008) 140-149.
- [4] Y. J. Feng, X. Y. Li, *Water Research*, **37** (2003) 2399-2407.
- [5] C. A. Martínez-Huitle, S. Ferro, *Chemical Society Reviews* **35** (2006) 1324.
- [6] M. Panizza, G. Cerisola, *Chemical Reviews* **109** (2009) 6541.
- [7] E. Chatzisyneon, S. Fierro, I. Karafyllis, D. Mantzavinosa, N. Kalogerakis, A. Katsaounis, *Catalysis Today* **151** (2010) 185–189.
- [8] Ch. Comninellis, *Electrochimica Acta* **39** (1994) 1857-1862.
- [9] S. Chai, G. Zhao, P. Li, Y. Lei, Y.-N. Zhang, D. Li, *Journal of Physical Chemistry C*, **115** (2011) 18261-18269.
- [10] S. Dutta, R. Chowdhury, P. Bhattacharya, *Indian Journal of Chemical Technology* **16** (2009) 7-16.
- [11] M. H. Entezari, C. Pétrier, P. Devidal, *Ultrasonics Sonochemistry* **10** (2003) 103-108.
- [12] S. Trasatti, *Electrochimica Acta* **45** (2000) 2377-2385
- [13] S. Trasatti (Ed.), *Studies in Physical and Theoretical Chemistry, Vol. 11: Electrodes of Conductive Metallic Oxides, Pt. A*, Elsevier Science Publishers, Amsterdam, Netherlands, 1980.
- [14] A. N. Subba Rao, V. T. Venkatarangaiah, *Environmental Science Pollution Research* **21** (2014) 3197–3217.
- [15] I. Sirés, E. Brillas, M. A. Oturan, M. A. Rodrigo, M. Panizza, *Environmental Science Pollution Research* **21** (2014) 8336-8367.
- [16] D. C. de Moura, C. K. C. de Araújo, C. L.P.S. Zanta, R. Salazar, C. A. Martínez-Huitle, *Journal of Electroanalytical Chemistry* **731** (2014) 145-152.
- [17] A. Kapalka, G. Foti, C. Comninellis, *Journal of Applied Electrochemical* **38** (2008) 7–16.
- [18] J. Iniesta, P. A. Michaud, M. Panizza, G. Cerisola, A. Aldaz, Ch. Comninellis, *Electrochimica Acta* **46** (2001) 3573-3578.
- [19] Ch. Comninellis and A. Nerini, *Journal of Applied Electrochemical* **25** (1995) 23–28.
- [20] Ch. Comninellis and E. Plattner, *Chimia* **42** (1988) 250–252.
- [21] E. V. Santos, S. F. M. Sena, D. R. Silva, S. Ferro, A. De Battisti, C. A. Martínez-Huitle *Environmental Science and Pollution Research* **21** (2014) 8466 – 8475.
- [22] C. A. Martínez-Huitle, M. A. Quiroz, C. Comninellis, S. Ferro, A. De Battisti, *Electrochim. Acta* **50** (2004) 949-956.
- [23] C. A. Martínez-Huitle, S. Ferro, A. De Battisti, *Electrochemical and Solid-State Letters* **8** (2005) D35 – 39.
- [24] M. Panizza, G. Cerisola, *Journal of Electroanalytical Chemistry* **32** (2010) 638-28
- [25] C. A. Martínez-Huitle, E. V. Santos, D. M. Araújo, M. Panizza, *Journal of Electroanalytical Chemistry* **674** (2012) 103–107.
- [26] J. H. Bezerra Rocha, M. M. Soares Gomes, E. Vieira dos Santos, E. C. Martins de Moura, D. Ribeiro da Silva, M. A. Quiroz, C. A. Martínez-Huitle, *Electrochimica Acta* **140** (2014) 419–426.
- [27] A. J. C. da Silva, E. V. dos Santos, C. C. de Oliveira Morais, C. A. Martínez-Huitle, S. S. L. Castro, *Chemical Engineering Journal* **233** (2013) 47.

- [28] A. Kapařka, L. Joss, A. Anglada, Ch. Comninellis, K. M. Udert, *Electrochemistry Communications* **12** (2010) 1714.
- [29] C. Indermuhle, M. J. Martín de Vidales, C. Sáez, J. Robles, P. Cañizares, J. F. García-Reyes, A. Molina-Díaz, Ch. Comninellis, M. A. Rodrigo, *Chemosphere* **93** (2013) 1720.
- [30] K. Juttner, U. Galla and H. Schmieder, *Electrochimica Acta* **45** 2000 2575–2594.
- [31] C. A. Martínez-Huitle, E. Brillas. *Angewandte Chemie International Edition* **47** (2008) 1998 – 2005.
- [32] A. M. Z. Ramalho, C. A. Martínez-Huitle, D. R. d Silva, *Fuel* **89** (2010) 531-534.
- [33] P. Canizares, J. Lobato, R. Paz, M. A. Rodrigo, C. Saez , *Water Research* **39** (2005) 2687–2703
- [34] Ch. Comninellis, A. De Battisti, *Journal Chimie Physique* **93** (1996) 673–679.
- [35] F. Bonfatti, S. Ferro, F. Lavezzo, M. Malacarne, G. Lodi, A. De Battisti, *Journal of the Electrochemical Society* **147** (2000) 592 - 596
- [36] F. Bonfatti, A. De Battisti, S. Ferro, G. Lodi, S. Osti, *Electrochimica Acta* **46** (2000) 305 - 314
- [37] A. Vacca, M. Mascia, S. Palmas, A. Da Pozzo, *Journal of Applied Electrochemical* **41** (2011) 1087–1097.
- [38] P. Cañizares, C. Sáez, A. Sánchez-Carretero, M.A. Rodrigo, *Journal of Applied Electrochemistry* **39** (2009) 2143.